Au L x-ray relative intensities induced by proton impact

J. Q. Xu*

Chinese Center of Advanced Science and Technology (World Laboratory), P.O. Box 8730, Beijing 100080, China and Shanghai Institute of Nuclear Research, Academia Sinica, P.O. Box 800–204, Shanghai 201800, China

(Received 8 March 1991)

Theoretical intensity ratios of the $L\beta$, $L\gamma$, $L\eta$, $L\gamma_1$, and $L\gamma_{2,3,6}$ to the $L\alpha$ line induced by proton impact on gold have been calculated from various L-subshell databases in the proton energy range 0.18–10 MeV. Good agreements are obtained between the measurements and the ratios computed by using the decay yields we present and the ionization cross sections by Cohen and Harrigan [At. Data Nucl. Data. Tables **33**, 255 (1985)]. The latter were calculated in the plane-wave Born approximation with corrections for energy loss, Coulomb deflection, perturbed stationary state, and relativistic effects. The L-subshell coupling effects are not found.

In the past decade many publications reported and discussed the so-called L_2-subshell-related discrepancies, i.e., the noticeable difference between theoretical ratios of the $L\gamma$ to $L\alpha$ line intensities (or the L_2 to L_3 subshell ionization cross sections) and experimental data for heavy projectile impact on high-Z elements [1–8]. The $L\gamma_1$ transition to the L_2 subshell is a major component of the $L\gamma$ transition. One of the theories used for calculation of ionization cross sections for heavy charged particles, published in 1981 by Brandt and Lapicki [9], uses the plane-wave Born approximation (PWBA) with corrections for particle-energy loss (E), Coulomb deflection (C), perturbed stationary state (PSS), and relativistic effects (R), and is abbreviated ECPSSR. Since then, the theory has been examined by a large number of experiments and found wide applications in atomic physics, proton-induced x-ray emission (PIXE) analyses, and so forth. Hence Cohen and Harrigan presented in 1985 and in 1986 the ECPSSR tables for K- and L-shell ionization cross sections [10] and for relative L-subshell x-ray intensities [2] by means of the fluorescence and Coster-Kronig yields semiempirically compiled by Krause [11] and the L-subshell emission rates fitted by Salem [12].

Another theory for calculation of ionization cross sections, published in 1982 and 1985 by Chen, Crasemann, and Mark [8] and Chen and Crasemann [13], uses the relativistic plane-wave Born approximation (RPWBA) with Dirac-Hartree-Slater (DHS) wave functions. Semiclassical corrections for binding-energy, polarization, and Coulomb deflection (BC) were included. Their more extensive tables have been given recently for incident proton energies from 1 to 5 MeV [14]. As the energy decreases below about 1 MeV, this theory fails in comparison with measurements.

In addition, Scofield reported in 1974 the DHS and Dirac-Hartree-Fock (DHF) x-ray emission rates [15,16]. The former were tabulated in detail and widely used, but the latter were more favorable when compared with measurements. The DHF value tables have also been presented by Campbell and Wang [17] recently.

In 1988, Campbell [18] made a comparison between the ECPSSR and the DHS x-ray intensity ratios of major L line groups, $I(L\beta)/I(L\alpha)$ and $I(L\gamma)/I(L\alpha)$, of gold in proton energy region between 1.0 and 3.0 MeV. The latter ratios were calculated from the RPWBA-DHS-BC cross sections, the DHS fluorescence and Coster-Kronig yields of Chen, Crasemann, and Mark [19] and the DHF emission rates. Then he concluded that the DHS intensity ratios were in good agreement with experimental data compiled by Sokhi and Crumpton [20] while the ECPSSR ratios of Cohen and Harrigan [2] were in worse agreement. However, as pointed out by Harrigan and Cohen [21], the L_2-related effects are particularly important only below ~ 0.5 MeV.

Many efforts have been devoted to the explanation of the anomalous L_2-related behavior and failed in success [2–6,21]. Recently Sarkadi and Mukoyama [3] ascribed it to the effect of L-subshell coupling on the L-subshell ionization cross sections, which takes place through a secondary interaction between the projectile and the target electrons and is better tested for ions heavier than protons and helium [5,22]. The effect increases with the atomic number of the projectile and is expected to be weak for protons. However their calculations indicated that the coupling effect was particularly large for the L_2 subshell, reaching 40% at proton energy $E_p \approx 0.25$ MeV for gold [3]. Using these correction factors they modified the RPWBA-DHS-BC cross sections but the agreement between their calculations and the measurements of Jitschin *et al.* [1] was still rather poor, reaching the deviation of an average 35% and of 20% at large proton energies in the region $0.175 \leq E_p \leq 10$ MeV [3].

In this work, we will attribute the L_2-related discrepancies to the L-vacancy decay yields only and clearly verify that the ECPSSR theory can describe satisfactorily the measurements [1,20] for proton impact on Au if the decay yields we present here are adopted. The present study is restricted to proton impact since clearly in the case of heavier projectiles, some complicated effects due to the multiple-vacancy production and the L-subshell coupling should be taken into account.

Recently, we acquired the L-subshell fluorescence

TABLE I. Au L-subshell fluorescence and Coster-Kronig yields.

	ω_1	ω_2	ω_3	f_{12}	f_{13}	f_{23}	Reference
Krause	0.107	0.334	0.320	0.14	0.53	0.122	[11]
Chen, Crasemann, and Mark[a]	0.0822	0.363	0.320	0.07	0.701	0.128	[19]
Campbell and McGhee		0.342	0.286			0.112	[26]
		±0.010	±0.007			± 0.004	
Werner and Jitschin	0.137		0.307	0.047	0.582	0.101	[27]
	±0.008		±0.012	±0.020	±0.010	±0.010	
Xu	0.121	0.355	0.296				[23]
	±0.012	±0.018	±0.012				
Present				0.12	0.56	0.12	

[a]Data for gold are reported in Ref. [18].

yields [23] ω_i ($i=1$, 2, and 3), of elements around the atomic number $Z=80$ from the L-series x-ray spectra induced by electron impact and recorded with a curved-crystal spectrometer [24] based on a model for heavy elements that is generally similar to our previous model [25]. These ω_1 values, which agree well with recent measurements [26,27], are approximately 20% larger than the compiled data of Krause [11] and 55% larger than the DHS calculations of Chen, Crasemann, and Mark [19] for the elements with $Z \approx 80$. The values are listed in Table I.

As pointed out in many articles, most L-subshell ionization cross sections for particle impact were published only as final values that were calculated from directly measured L x-ray intensities and some selected database; so these experimental cross sections have been already more or less distorted. Therefore, we preferred to treat relative intensities, and calculated the ratios of individual lines and major L line groups to the $L\alpha$ line in the following three cases. In case A, the results were computed by using the ECPSSR cross sections and the compiled fluorescence and Coster-Kronig yields [11]. In case B, our fluorescence yields (Table I) were adopted; the others are the same as in case A. In case C, the DHS data [14,19] were used. The present work is based on gold, for which a number of experimental data exist [20], with sufficient consistency in the region $0.5 < E_p < 3$ MeV.

The x-ray-production cross sections of the $L\rho$ line are

TABLE II. Case B ECPSSR intensity ratios of Au $L\beta$, $L\gamma$, $L\gamma_1$, and $L\gamma_{2,3,6}$ to $L\alpha$ line induced by protons of energy E_p (in MeV). The values are computed by using the ECPSSR ionization cross sections (Ref. [10]), Xu's fluorescence and Krause's Coster-Kronig yields (Table I), and the DHF x-ray emission rates (Ref. [17]). The data in parentheses are obtained by using the present Coster-Kronig yields (Table I) instead.

E_p	I_β/I_α	I_γ/I_α	I_{γ_1}/I_α	$I_{\gamma_{2,3,6}}/I_\alpha$
0.18			3.22×10^{-2}	4.91×10^{-2}
		(0.0872)	(2.96)	(4.83)
0.20	0.562	0.0926	3.39	4.92
	(0.548)	(0.0890)	(3.13)	(4.84)
0.30	0.565	0.0914	3.89	4.38
	(0.552)	(0.0883)	(3.66)	(4.32)
0.50	0.541	0.0818	4.43	3.10
	(0.533)	(0.0798)	(4.27)	
0.70	0.527	0.0756	4.83	2.23
	(0.521)	(0.0743)	(4.73)	
1.0	0.522	0.0721	5.34	1.49
1.5	0.538	0.0747	5.97	1.16
2.0	0.564	0.0814	6.39	1.36
2.5	0.590	0.0888	6.68	1.73
3.0	0.614	0.0956	6.90	2.13
3.5	0.635	0.1015	7.08	2.48
4.0	0.652	0.1065	7.22	2.78
	(0.646)	(0.105)	(7.09)	
4.4	0.664	0.110	7.32	2.98
	(0.657)	(0.108)	(7.18)	
7.0			7.83	3.73
	(0.704)	(0.122)	(7.63)	(3.69)
9.4			8.13	4.00
	(0.726)	(0.128)	$(7.92)\times10^{-2}$	$(3.95)\times10^{-2}$

given by

$$\sigma_\rho(L_1)=\sigma_1\omega_1\Gamma_\rho/\Gamma_R(L_1)\ ,$$

$$\sigma_\rho(L_2)=(\sigma_2+\sigma_1 f_{12})\omega_2\Gamma_\rho/\Gamma_R(L_2)\ ,$$

$$\sigma_\rho(L_3)=\frac{[\sigma_3+\sigma_2 f_{23}+\sigma_1(f_{13}+f'_{13}+f_{12}f_{23})]\omega_3\Gamma_\rho}{\Gamma_R(L_3)}\ ,$$

where σ_i is the L_i-subshell ionization cross section; f'_{13} is the L_1 to L_3 intrashell radiative yield, which is much smaller than the Coster-Kronig yields f_{ij} for gold. In the three cases, we used Krause's value $f'_{13}=0.0028$. Here Γ_ρ and $\Gamma_R(L_i)$ are the L_ρ-line and L_i-subshell radiative widths, respectively. In this work, we used the DHF values [17] of Γ_ρ and $\Gamma_R(L_i)$. For thin targets, the relative intensity between the $L\rho$ and $L\alpha$ lines is given by

$$I_\rho/I_\alpha=\sigma_\rho/\sigma_\alpha\ ,$$

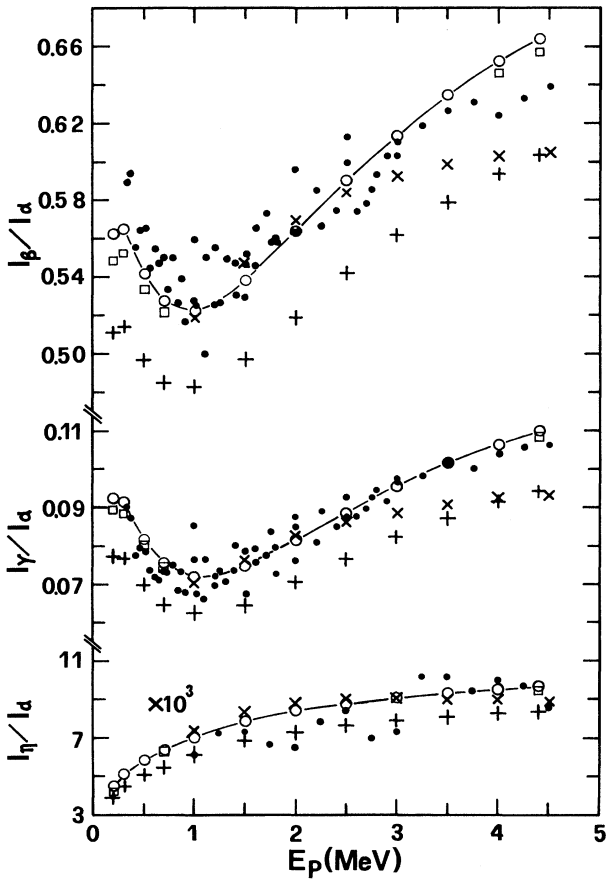

FIG. 1. Intensity ratios of Au $L\beta$, $L\gamma$, and $L\eta$ to $L\alpha$ line as a function of proton energy E_p. The small dots are experimental data (Refs. [20] and [28]). Theoretical data: +, computed by using the ionization cross sections σ_i(ECPSSR) and Krause's fluorescence and Coster-Kronig yields (Ref. [11]); ○, by using the σ_i(ECPSSR), our fluorescence and Krause's Coster-Kronig yields; □, by using the σ_i(ECPSSR) and our fluorescence and Coster-Kronig yields (see Table I); ×, by using the DHS (RPWBA-BC) cross sections and decay yields (Refs. [14] and [19]).

where ρ denotes $\beta,\gamma,\eta,\gamma_1$, etc. From the above expressions, we know that the ratio I_ρ/I_α depends essentially upon the ionization cross sections and the fluorescence yields when $E_p>0.3$ MeV because the Coster-Kronig yields are all much less than unity and in small terms in the related sums.

The ratios of I_β/I_α, I_γ/I_α, and I_η/I_α computed in the three cases are given in Fig. 1, together with the experimental data collected from the literature [20,28]. The ECPSSR values calculated in case B are also listed in Table II. Here the $L\alpha$, $L\beta$, and $L\gamma$ lines denote $L\alpha_{1,2}$, $L\beta_1$ to $L\beta_7$ and $L\beta_{15}$, and $L\gamma_1$ to $L\gamma_6$ and $L\gamma_8$, respectively. Figure 1 shows that the ECPSSR intensity ratios of case B (circles) are in good agreement with the experimental data and are by far the best of the three theoretical ratios. The ECPSSR values in case A are systematically about 10% lower than the new ones, which should be ascribed to the different fluorescence yields adopted in the two cases. The DHS intensity ratios obtained in case C agree well with the case B ECPSSR ones for proton energies from 1 to 2.5 MeV, but are a little lower when the energy goes beyond this region. When the energy reaches about 4 MeV, the DHS ratios approximate the case A ECPSSR values. In addition, we must bear in mind that the DHS fluorescence yields for gold are notably different from the measurements (see Table I).

In order to study the relative intensities still further, we plotted the ratios of I_{γ_1}/I_α and $I_{\gamma_{2,3,6}}/I_\alpha$ computed in cases B and C, and the measurements of Jitschin *et al.* [1] in Fig. 2. The agreement between the case B ECPSSR values and the measurements is very good, at least for $E_p\geq 0.25$ MeV. The case B ECPSSR ratios of I_{γ_1}/I_α are nearly on a straight line, whereas the ratios of $I_{\gamma_{2,3,6}}/I_\alpha$ appear a minimum at $E_p\approx 1.5$ MeV, responding to the nodal structure of the $2s$ wave function.

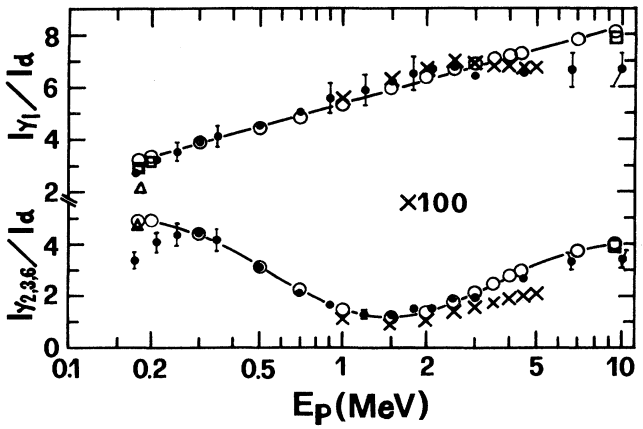

FIG. 2. Intensity ratios (×100) of Au $L\gamma_1$ and $L\gamma_{2,3,6}$ to $L\alpha$ line as a function of proton energy E_p. The experimental data (small dots, with typical error bars) are from Jitschin *et al.* (Ref. [1]). The triangles are calculated by using the ECPSSR ionization cross sections (Ref. [10]), and our fluorescence (Table I) and Werner's Coster-Kronig yields (Ref. [27]). For definition of the other symbols, see the caption to Fig. 1.

We attribute the small deviation of the calculated I_{γ_1}/I_α from the measurements at the very low energies to the use of Krause's Coster-Kronig yields. As pointed out in a recent article of the author [23], Krause's compilation overestimated more or less the f_{12} and underestimated the f_{13} for elements around $Z=80$. Here, we propose $f_{12}=0.12$, $f_{13}=0.56$, and $f_{23}=0.12$ by analyses of experimental data reported in recent years. Using the Coster-Kronig yields instead of Krause's, we made calculations in case B and plotted the results in the two figures (squares). The agreements of the calculated I_{γ_1}/I_α and I_γ/I_α with the measurements are improved at the low energies. We regard the excellent agreements as the most success so far in explanations of the L_2-related discrepancies. The L-subshell coupling effects are not found (or too weak to be found) in the region $0.175 \leq E_p \leq 10$ MeV. The ratios calculated at $E_p=0.18$ MeV in case B by using the Coster-Kronig yields of Werner and Jitschin [27] are also given in Fig. 2. We found that the I_{γ_1}/I_α (triangle) was even smaller.

In this paper, no attempt was made to study the deviations of the theoretical $I_{\gamma_{2,3,6}}/I_\alpha$ and I_β/I_α from the measurements at the low energies because both ratios are mainly related to the L_1-subshell with higher binding energy. However, the figures show that the experimental data of the $I_{\gamma_{2,3,6}}/I_\alpha$ are less than the calculations, whereas the data of the I_β/I_α are more than the calculations, so that new measurements in this energy region are needed.

This work was supported by the National Natural Science Foundation of China.

*Permanent address: Shanghai Institute of Nuclear Research, Academia Sinica, P.O. Box 800–204, Shanghai 201800, China.

[1] W. Jitschin, A. Kaschuba, R. Hippler, and H. O. Lutz, J. Phys. B **15**, 763 (1982).
[2] D. D. Cohen and M. Harrigan, At. Data Nucl. Data Tables **34**, 393 (1986).
[3] L. Sarkadi and T. Mukoyama, Phys. Rev. A **37**, 4540 (1988).
[4] D. D. Cohen, Nucl. Instrum. Methods B **49**, 1 (1990).
[5] L. Sarkadi and T. Mukoyama, J. Phys. B **14**, L255 (1981); Nucl. Instrum. Methods B **4**, 296 (1984); T. Mukoyama and L. Sarkadi, Nucl. Instrum. Methods **190**, 619 (1981); **205**, 341 (1983); **211**, 525 (1983); T. Papp, J. Pálinkás, L. Sarkadi, B. Schlenk, I. Török, and K. Kiss, Nucl. Instrum. Methods B **4**, 311 (1984); L. Sarkadi, J. Phys. B **19**, L755 (1986).
[6] D. D. Cohen, Nucl. Instrum. Methods **218**, 795 (1983); Nucl. Instrum. Methods B **3**, 47 (1984); D. D. Cohen and M. Harrigan, Nucl. Instrum. Methods B **15**, 576 (1986).
[7] M. Vigilante, P. Cuzzocrea, N. De Cesare, F. Murolo, E. Perillo, and G. Spadaccini, Nucl. Instrum. Methods B **51**, 232 (1990); J. Braziewicz, M. Pajek, E. Braziewicz, J. Ploskonka, and G. M. Osetynski, *ibid.* **15**, 585 (1986).
[8] M. H. Chen, B. Crasemann, and H. Mark, Phys. Rev. A **26**, 1243 (1982).
[9] W. Brandt and G. Lapicki, Phys. Rev. A **23**, 1717 (1981).
[10] D. D. Cohen and M. Harrigan, At. Data Nucl. Data Tables **33**, 255 (1985).
[11] M. O. Krause, J. Phys. Chem. Ref. Data **8**, 307 (1979).
[12] S. I. Salem, S. L. Panossian, and R. A. Krause, At. Data Nucl. Data Tables **14**, 91 (1974).
[13] M. H. Chen and B. Crasemann, At. Data Nucl. Data Tables **33**, 217 (1985).
[14] M. H. Chen and B. Crasemann, At. Data Nucl. Data Tables **41**, 257 (1989).
[15] J. H. Scofield, At. Data Nucl. Data Tables **14**, 121 (1974).
[16] J. H.Scofield, Phys. Rev. A **9**, 1041 (1974); **10**, 1507 (1974); **12**, 345 (1975).
[17] J. L. Campbell and J. X. Wang, At. Data Nucl. Data Tables **43**, 281 (1989).
[18] J. L. Campbell, Nucl. Instrum. Methods B **31**, 518 (1988).
[19] M. H. Chen, B. Crasemann, and H. Mark, Phys. Rev. A **24**, 177 (1981).
[20] R. S. Sokhi and D. Crumpton, At. Data Nucl. Data Tables **30**, 49 (1984).
[21] M. Harrigan and D. D. Cohen, Nucl. Instrum. Methods B **15**, 581 (1986).
[22] P.A. Amundsen and D. H. Jakubassa-Amundsen, J. Phys. B **21** L99 (1988).
[23] J. Q. Xu, Phys. Rev. A **43**, 4771 (1991).
[24] M. Goldberg, Ann. Phys. (Paris) **7**, 329 (1962).
[25] J. Q. Xu and E. Rosato, Phys. Rev. A **37**, 1946 (1988); J. Q. Xu, J. Phys. B **23**, 1423 (1990); J. Q. Xu and E. Rosato, J. Phys. (Paris) Colloq. **48**, C9-661 (1987).
[26] J. L. Campbell and P. L. McGhee, J. Phys. (Paris) Colloq. **48**, C9-597 (1987).
[27] U. Werner and W. Jitschin, Phys. Rev. A **38**, 4009 (1988).
[28] A. P. Jesus, T. M. Pinheiro, I. A. Niza, J. P. Ribeiro, and J. S. Lopes, Nucl. Instrum. Methods B **15**, 595 (1986).